International Journal of Engineering Research and Technology. ISSN 0974-3154 Volume 10, Number 1 (2017)

Electrochemical supercapacitor properties of SnS thin films deposited by low-cost chemical bath deposition route

A. M. Patil
Thin Film Physics Laboratory, Department of Physics, Shivaji University, Kolhapur, 416004 (M.S), India

A. C. Lokhande
Department of Materials Science and Engineering, Chonnam National University 300 Yongbong-Dong, Puk-Gu, Gwangju, South Korea

P. A. Shinde
Thin Film Physics Laboratory, Department of Physics, Shivaji University, Kolhapur, 416004 (M.S), India

H. D. Shelke
Thin Film Physics Laboratory, Department of Physics, Shivaji University, Kolhapur, 416004 (M.S), India

C. D. Lokhande
Centre for Interdisciplinary Research, D. Y. Patil University, Kolhapur.

Abstract
In this work, the microflowers like surface morphological SnS thin film material prepared by simple, convenient and inexpensive chemical bath deposition method. The structural analysis shows orthorhombic crystal structure of all the SnS thin films prepared at different deposition time period. The electrochemical supercapacitive properties of all the electrode materials are investigated in 2 M KOH electrolyte. The maximum specific capacitance of 1375 Fg^{-1} is achieved for SnS thin film at a deposition time of 1 h. The highest energy density and power density of 60 Wh kg^{-1} and 8 KW kg^{-1} is achieved, respectively for SnS thin films.

Keywords:chemical bath deposition, thin film, SnS, electrochemical supercapacitor

Introduction

In electric energy storage, supercapacitor received great attention due to its vital properties like higher power density (SPD) than batteries and more energy density (SED) than conventional capacitors. However, supercapacitors have additional advantages over batteries such as longer cycling life, simple fabrication, inexpensive and requirement of simple electric circuit mechanism [1-3]. The use of supercapacitors with batteries at the period of braking in hybrid electric vehicles provide the higher electric power during acceleration. The charge storage mechanism divides supercapacitor in to two categories as; electrochemical double layer capacitor (EDLC) and pseudocapacitor. The charge storage in EDLC type supercapacitor is due to the reversible adsorption of cations as well as anions at the electrode-electrolyte interface, while in pseudocapacitor charge storage belongs to fast surface redox reactions of the electrode with the electrolyte ions [4, 5]. Presently, the highly porous carbon materials are used in commercial EDLCs because of the higher surface area of the porous carbon electrodes which increases the interaction of electrolyte ions and the electrode material [6, 7]. In contradict, the synthesis process of carbon materials is difficult and expensive. Therefore, the inexpensive, easily available and electrical conductive stainless steel (SS) material is suitable as a substrate material in supercapacitor application. In other side, the electrode material which has higher electrochemical efficiency and ability to store more electric charges per unit area are required for supercapacitor.

Generally, carbon material [9], metal oxide and chalcogenide nanoparticles [10] or their nanocomposites [11, 12] have been explored as electrode materials for supercapacitor. Nevertheless, Sn-based metal chalcogenide materials like SnS, SnS2, SnSe, etc. are used for various applications due to their excellent optical and electrochemical properties such as solar cell [13], supercapacitor [14], and lithium ion batteries [15]. But these materials have not been extensively examined as supercapacitor materials, while they are broadly used as electrode material for lithium ion batteries because of large volume expansion. From various phases of tin sulfide, the tin monosulfide (SnS) thin films are more important in the view of solar cell and supercapacitor [16]. The phase of SnS holds two layers per unit cell, in which one is along with elongated distance ‘S’ atom among the adjacent layers. This layer is important because of the arrangement of cations and anions of SnS is depends on this type of layer and the cations layer detached by weak van der Waals forces [14]. The layer of SnS thin film provides the intercalation with cationic ion of electrode material, which helps to improve the electrochemical supercapacitor performance of SnS electrode material. The properties of SnS like high absorption coefficient, dual type semiconductor and lower toxic nature

fix the scope of SnS electrode in future electrode material fabrication. Also, the storage ability of SnS electrode material can be enhanced by the wide range of potential windows over some other metal chalcogenides (e.g NiS, MnS, CoS, MoS etc) [17].

In the present work, SnS thin films are successfully synthesized from simple, inexpensive, surfactant free and convenient chemical bath deposition (CBD) method. The time variation in the deposition effects on the surface morphology and other properties including electrochemical supercapacitor performance of electrode material. The basic characterization of prepared SnS electrode material carried out with different characterization techniques. The electrochemical supercapacitor properties of electrode material also studied using cyclic voltammetry (CV), galvonnostatic charge-discharge (GCD), electrochemical stability and electrochemical impedance spectroscopy analysis. In this way, obtained electrochemical values of SnS material is much better than previous reports [14, 17].

Experimental

Chemicals:

The tin chloride ($SnCl_2$), triethylamine (TEA), hydrochloric acid (HCl), potassium hydroxide (KOH) and sodium thiosulfate pentahydrate ($Na_2S_2O_3.5H_2O$) were used without further purification (Sigma Aldrich). The commercially available flexible SS material (304 grade) was used as current collector material.

Synthesis of SnS thin films:

In a typical synthesis, $SnCl_2$ and $Na_2S_2O_3$ were used as tin and sulfur sources, respectively, and TEA was used as a complexing agent. The cationic source of 0.1 M $SnCl_2$ dissolved in 50 ml DDW by continuous stirring using a magnetic stirrer. Four beakers of 50 ml were used for deposition of thin film at different time period. After dissolving of $SnCl_2$ in DDW, 1.5 ml of TEA was mixed drop wise in each beaker solution at stirring condition. Further, 0.2 M of $Na_2S_2O_3$ was added in the above solution for SnS thin film formation. Besides, dilute HCl was added drop wise in solution till pH becomes 4.5 (± 0.1). Afterward, the drop wise addition of HCl change the solution transparent light-yellow. These beakers were placed in a constant temperature bath which is maintained at constant temperature of 353 K.

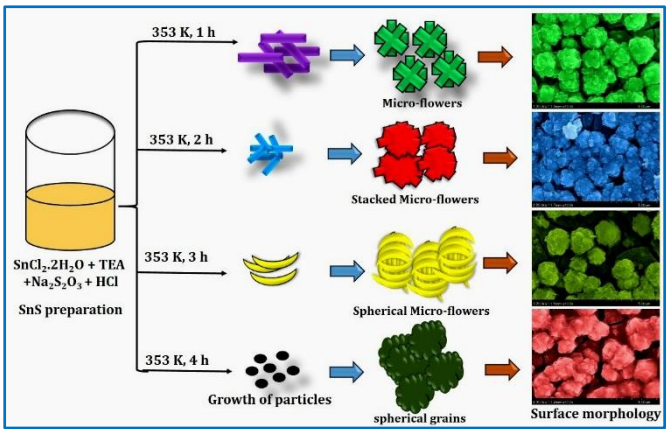

Schematic.1 Schematic representation of formation of SnS thin films by CBD method.

The deposition of SnS thin films takes place after 1 h. The four beakers were takeout at 1, 2, 3 and 4 h time period. The deposition time alters the surface morphology of SnS thin films.

Results and discussion

The SnS thin films on SS substrate is deposited by CBD method. Deposition takes place with different stages of film formation, such as nucleation aggregation, coalescence and growth (Schematic 1). From 0.1 M $SnCl_2$ solution, Sn^{2+} ions are released and form complex with TEA (Equation. 1 and 2). The sulfur ions source gives H_2S in DDW (Equation. 3). The complex of Sn^{+2} ions with TEA and H_2S react in acidic (pH = 4.5 (±0.01) and SnS thin film is deposited on a SS substrate (Equation. 4).

$$Sn_4Cl_2.2H_2O + H_2O \rightarrow Sn^{2+} + Cl_2^{2-} + 3H_2O \quad (1)$$

$$Sn^{2+} + Cl_2^{2-} + TEA \rightarrow [Sn[TEA]]^{2+} + Cl_2^{2-} \quad (2)$$

$$Na_2S_2O_3 + H_2O \rightarrow H_2S + Na_2SO_4 \quad (3)$$

$$[Sn[TEA]]^{+} + H_2S + HCl \rightarrow SnS + TEA + HCl + 2H^{+} \quad (4)$$

At a temperature of 353 K well an adherent thin film is developed on SS substrate. After 1 h SnS deposited on SS substrate. The deposition time of 1, 2, 3 and 4 h gives SnS1, SnS2, SnS3 and SnS4 thin films, respectively.

Structural studies

The XRD pattern of CBD prepared SnS1, SnS2, SnS3 and SnS4 thin films is shown inFigure 1 (A). The high intense peaks observed at (011), (012), (102), (110), (013), (104), (022) and (115) crystalline planes which well match with JCPDS card no. 00-001-0984. The observed peak positions and crystal planes belongs to the formation of orthorhombic structure for all SnS thin films. The microstructure and growth direction of SnS thin film can be controlled by reaction time and nucleation rate. At reaction time of 1 and 2 h the strong diffraction peaks are observed at (013), (104) and (115) planes. The drop in intensity of peaks at reaction time of 3 and 4 h (SnS3 and SnS4) indicates restricted growth along x and y-axes. The SnS material deposited at four different deposition time confirms same plane peak positions, which implies that the high purity of SnS thin films. The reports obtained in this work well matches to literature [18-20]. XRD analyses reveal that the rise in crystalline size with an increase in deposition time up to a certain limit. The decrease of crystalline size is may be due to the quicker nucleation rate at higher time.

FT-IR studies

Figure 1 (B)displays FT-IR spectra of SnS thin films synthesized at four different deposition time. The peaks appeared in wave number of 640, 1440, 1640 and 3650 cm^{-1} strongly support to the formation of SnS material on SS substrate. The chemical composition of SnS microflowers was scrutinized by using FT-IR spectroscopy. The well-defined absorption bands were observed in the spectrum at 640, 1440

and 1640 cm^{-1}. The peak observed at 640 cm^{-1} in the spectrum is due to the development of Sn–S bond [21]. The two very weak peaks at 1440 and 1640 cm^{-1} are because of the formation of C–H and C–O bands, respectively [22]. Above peak analyses confirm that the thin film material is SnS. The peak observed at 3650 cm^{-1} related to stretching mode, which attributed to the hydroxyl group.It is clearly observed that the intensity and perceptiveness of peaks drop with increase in deposition time. High intensity of peaks at the higher deposition time mentions a number of functional groups in addition to better adherence of SnS thin film.

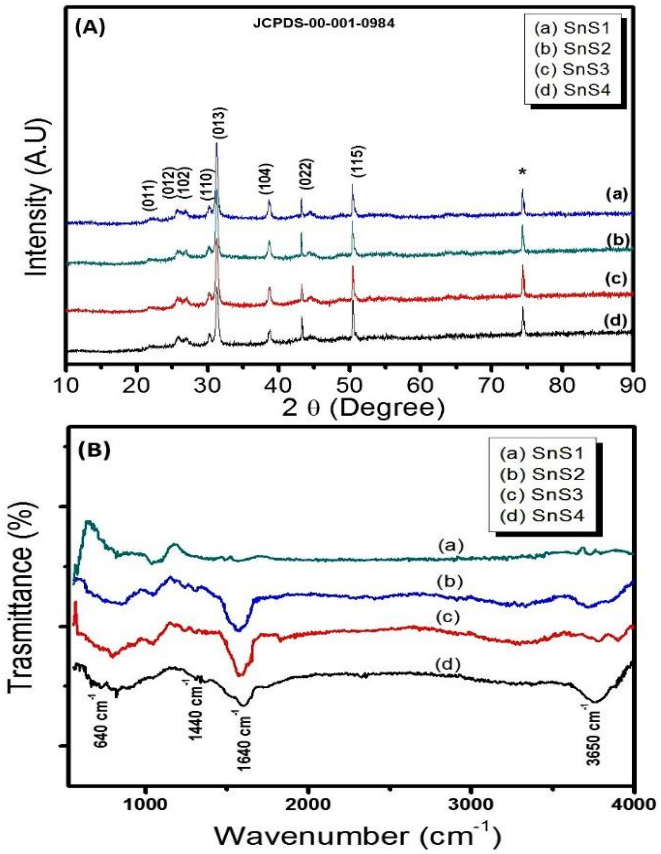

Figure 1: (A) The XRD patterns of (a) SnS1, (b) SnS2, (c) SnS3, and (d) SnS4 thin films, respectively, and (B) The FT-IR spectrum of (a) SnS1, (b) SnS2, (c) SnS3, and (d) SnS4 thin films, respectively.

Surface morphological studies

Figure 2 (A-H) shows the surface morphology of SnS thin films deposited at four different deposition time at reaction temperature of 353 K on SS substrates at two different magnifications of 10 and 20 K. The compactness of SnS surface increase up to a certain limit, then it decreases with increase in deposition time. The SnS1 thin film shows flowers like morphology. The average diameter of each flower is about 2 µm in size (Figure 2 (A, B)). As the deposition time increases, the slight increase in compactness with reduced size of micro flower is observed. Which gives less surface interaction with the electrolyte ions than NiS1 thin film.The growth of micro-flowers on SS substrate is uniform with moderately porous surface. As the deposition time increases the growth rate of reaction rises with the nucleation rate of thin film formation and surface becomes inactive with overgrowth of material on a SS substrate(Figure 2 (C, D)).The change in growth rate and direction of film formation implies that the deposition time is a tool to alter the morphology of SnS film surface. The diameter of micro-flower decreased bythe deposition time. The average size of stacked micro-flower (SnS3) is about 1.7 µm (Figure 2 (E, F)). Furthermore, the stacked micro-flowers are resized to spherical grain like structure at the deposition time of 3 h. The average size of spherical grains is about 1.5 µm. The outer nano-flakes are diminished with higher deposition time at reaction temperature of 353 K. Afterwards, at the deposition time of 4 h, spherical grains interconnect with each other. The compactness decreases at this condition, but the adherence of thin film material drops at for SnS4 thin film material. From above results, the SnS1 thin film material shows higher electrochemical properties with a more electroactive material contribution. The micro-flowers offer more specific surface area in electrochemical reaction [23, 24]. In summary, the SnS1 material is beneficial for further electrochemical supercapacitor investigations.

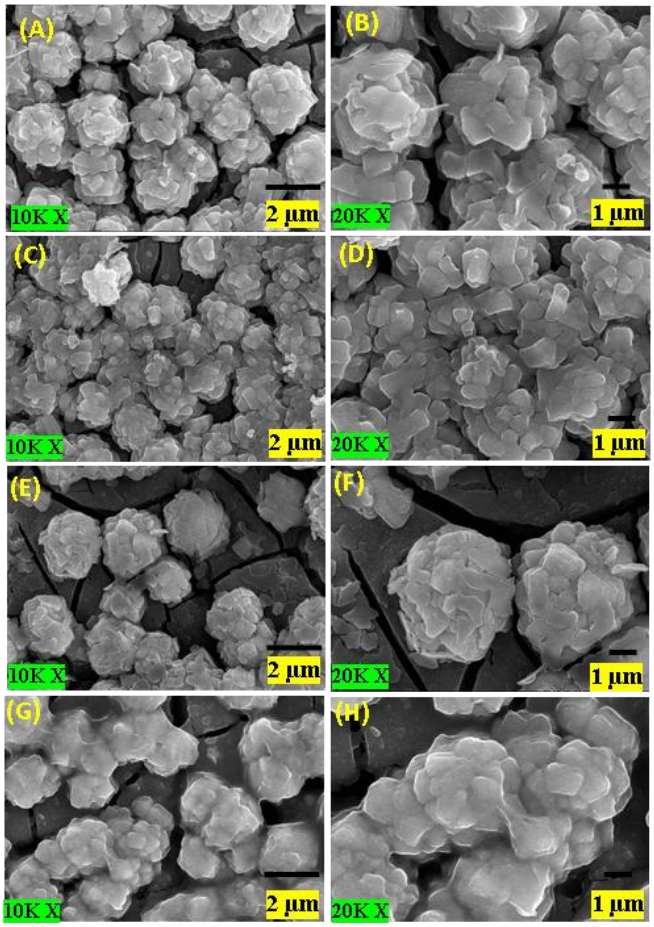

Figure 2: The FE-SEM images of (A and B) SnS1, (C and D) SnS2, (E and F) SnS3 and (G and H) SnS4 thin films at two different magnifications of 10000 X and 20000 X, respectively.

BET surface area study

The N_2 adsorption-desorption isotherm of SnS1 powder

sample is depicted in Figure 3 (A). The micro-flower like structure of SnS1 thin film is visualized by isotherm curves of type IV through the H3 hysteresis loop [25]. The corresponding BJH plot is represented in Figure 3 (B). The peak positions at 3.05, 5.5, 12.3, 19.6, 23.4 and 33.4 nm in pore size distribution graph expose the mesoporous range of the pores. The BET surface area observed in SnS1 sample is about 86.6 m^2 g^{-1}. Chauhan et al. [14] prepared SnS nanoparticles using the solvothermal route for applications in supercapacitor devices and reported specific surface area of 221 m^2 g^{-1}. Results obtained from BET analysis is correlated with FE-SEM analysis. The micro-flowers show higher surface area with a smallest pore size of 3.05 nm. The greater specific surface area of SnS thin film is beneficial for electrochemical supercapacitor application [26]. The peaks in the pore size distribution plot between 3 to 34 nm indicates that the different sized mesoporous SnS thin film distribution the thin film material. This type of pore size distribution of material provides larger electroactive SnS material in electrochemical reaction of electrode with electrolyte.

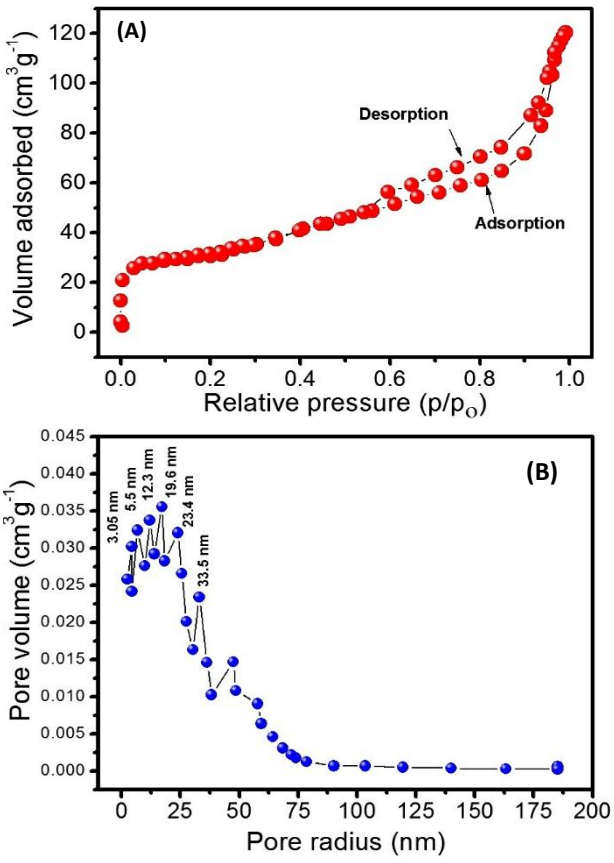

Figure 3:(A) The N_2 adsorption-desorption isotherms of SnS1 thin film, and (B) Pore size distribution plot of SnS1 powder sample.

Contact angle measurements

The interfacial contact properties between SnS thin film electrodes and aqueous electrolyte is determined by contact angle measurement. The water contact angle of SnS1, SnS2, SnS3 and SnS4 thin films are included in inset Figure 4. These thin films show contact angles of 38, 45, 56 and 65°, respectively. SnS1 thin film gives lower contact angle which confirms hydrophilic nature of electrode material, which is beneficial to enhance the electrochemical supercapacitive performance of electrode.

Thickness measurements

Thickness of thin film can be change the surface properties of thin film material. Figure 4 displays thickness of SnS1, SnS2, SnS3 and SnS4 thin films deposited at deposition time period of 1, 2, 3 and 4 h, respectively. It shows thickness of 575, 702, 754 and 603 nm for SnS1, SnS2, SnS3 and SnS4 thin films, respectively. As deposition time increases, the thickness also increase up to 3 h. After that due to overgrowth of material on substrate, the film shows reduction in thickness for SnS4 thin film.

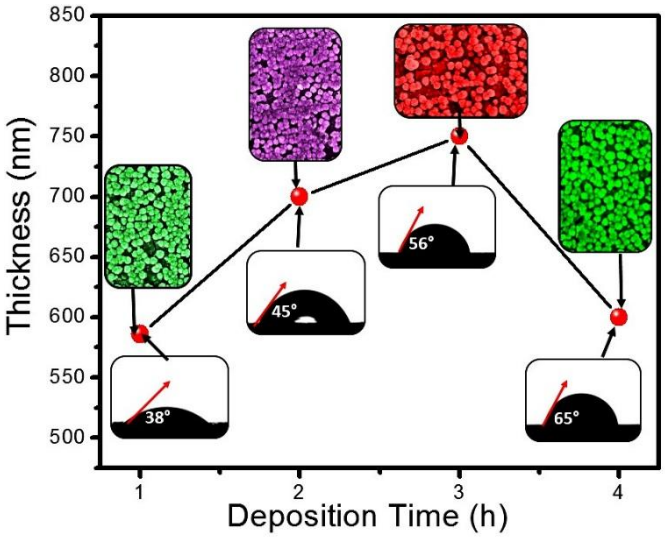

Figure 4: Thickness versus deposition time plot of SnS1, SnS2, SnS3 and SnS4 thin films (Inset figure shows water contact angles and surface morphology of SnS1, SnS2, SnS3 and SnS4 thin film

Supercapacitive properties

Cyclic Voltammetry (CV)

The surface morphology and structure of thin film material mainly impact on the electrochemical performance [27]. The microstructure of the surface of electrode provides a larger surface area of electroactive material. This type of surface allows better intercalation of electric charges in electrode material. The deposition time alters the surface morphology as well as the electrochemical performance [28].Therefore, the SnS1, SnS2, SnS3 and SnS4 electrodes have been employed to CV, GCD and EIS tests to investigate the deposition temperature influence on the electrochemical supercapacitor performance SnS thin films and to choose the optimized high performance condition for electrode preparation.

The CV evaluations are carried out for SnS1, SnS2, SnS3 and SnS4 electrodes in the potential windows of -0.5 to -1.2 V/SCE in 2 M KOH electrolyte. Usually, metal sulfide electrodes in the alkaline electrolytes store charges at the

interface of the electrode/electrolyte and in the bulk of electrode material [29]. Figure 5(A-D) depicts the CV curves of SnS1, SnS2, SnS3 and SnS4 electrode at a scan rates of 5, 10, 20, 50 and 100 mV s^{-1}.Figure 5 (E)shows comparative CV curves of all four electrodes at fix scan rate of 100 mV s^{-1}. The CV curves show the precise redox peaks at the potential positions of -0.7 and -1.05 V/SCE confirms that the charge storage due to redox reactions rather than EDLC. The kinetic irreversibility of electrode gives asymmetry on the both sides, i.e oxidation and reduction sides of CV curves [30]. The charge storage in the SnS electrode material is on the basis of following reaction,

$$SnS + OH^- \leftrightarrow SnSOH + e^- \quad (5)$$

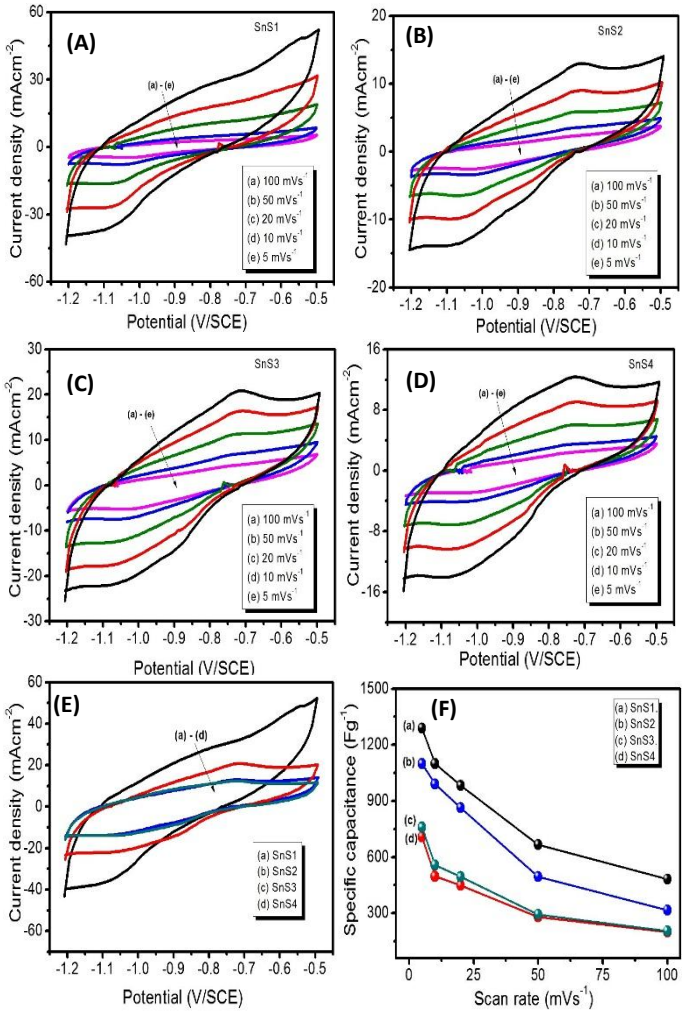

Figure 5: The CV curves recorded at different scan rate for (A) SnS1, (B) SnS2, (C) SnS3 and (D) SnS4 electrodes, respectively, (E) the comparative CV curves of all electrodes at 100 mV s^{-1}scan rate, and (F) the specific capacitance versus scan rate plot of all SnS thin films.

From these CV curves it is clearly seen that the area under CV curves for SnS1 micro-flower electrode material is higher than other electrode. In that way, the SnS1 electrode is preferred as the higher performance electrode material. Furthermore, to confirm the better electrode material, the specific capacitance (C_s) is calculated such as [28],

$$Cs = \frac{1}{ms\,(V_1 - V_0)} \int_{V_0}^{V_1} I\,(V)\,dV \quad (6)$$

Where, 'C_s' is specific capacitance, 'm' is mass of deposited SnS material on 1 cm^2 area, 's' is scan rate, ($V_1 - V_0$) is potential window and 'I' is current response. The estimated values of specific capacitance for SnS1, SnS2, SnS3 and SnS4 electrodes as 1290, 1100, 759 and 708 F g^{-1} at scan rate of 5 mV s^{-1}. Figure 5(F)illustrates the C_s versus scan rate plots for SnS1, SnS2, SnS3 and SnS4 electrodes.The obtained Cs values are higher at alower scan rate due to the more time available to intercalate OH^- ions at lower scan rate (5 mV s^{-1}) than high scan rate (100 mV s^{-1}).At the higher scan rate only surface of electrode material contributes electrochemical reaction not in bulk of material, which gives a lower electrochemical performance. From all the SnS thin films, SnS1 electrode display more C_s values for all scan rates due to higher electroactive material accessibility [31].

Galvonostatic Charge-discharge (GCD) study

The GCD analysis is carried out for all four SnS electrodes at different current densities of 3, 4, 5 and 7 mA cm^{-2} between potential of -1.2 to -0.5 V/SCE in 2 M KOH electrolyte. Figure 6 (A-D) shows the charge-discharge curves for SnS1, SnS2, SnS3 and SnS4 electrodes, respectively. The results obtained from GCD curves confirms the capacitance contributed from pseudocapacitor as well as EDLC type[14]. The lower interface resistance (IR) drop is observed for SnS1 electrode (-0.5 to -0.73 V/SCE) as compared to SnS2 (-0.5 to -0.78 V/SCE), SnS3 (-0.5 to -0.81 V/SCE) and SnS4 electrodes (-0.5 to -0.83 V/SCE). The slope shaped curves after -0.8 V/SCE indicated the pseudocapacitor behavior of SnS electrode. The C_s values are calculated using following equation as,

$$Cs = \frac{I \times t}{m \times \Delta V} \quad (7)$$

Where, 'I' is the current density, 't' is discharging time, 'm' is a mass of material loaded at 1 cm^2 which is dipped in electrolyte and 'ΔV' is potential window. From GCD analysis, C_s values obtained for SnS1, SnS2, SnS3 and SnS4 electrodes as 1375, 1206, 688 and 350 F g^{-1}, respectively, at a constant current density of 3 mA cm^{-2}. The achieved values of specific capacitance is due to the micro-flower like structure of SnS thin film. The results reported in this work is much higher than other previous reports, it is due to the higher specific surface area, surface morphology and the electrical conductivity of SnS electrode[14, 32, 33]. Figure 6 (E) shows the comparative GCD curves of SnS1, SnS2, SnS3 and SnS4 electrodes. The greater discharging rate of the SnS1 electrode proves the more charge storage ability of SnS1 electrode. The comparatively higher material interaction of electrode material with the OH^- ions from KOH electrolyte is because of the more time available for charge transfer at a lower

current density. At a lower current density, the rate of intercalation is higher due to the total electrode material interaction. Also, the IR drop values for all electrodes increases with an increase in current density and the C_s values decreases correspondingly [34].

Galvonostatic Charge-discharge (GCD) study

The GCD analysis is carried out for all four SnS electrodes at different current densities of 3, 4, 5 and 7 mA cm^{-2} between potential of -1.2 to -0.5 V/SCE in 2 M KOH electrolyte. Figure 6 (A-D) shows the charge-discharge curves for SnS1, SnS2, SnS3 and SnS4 electrodes, respectively. The results obtained from GCD curves confirms the capacitance contributed from pseudocapacitor as well as EDLC type[14]. The lower interface resistance (IR) drop is observed for SnS1 electrode (-0.5 to -0.73 V/SCE) as compared to SnS2 (-0.5 to -0.78 V/SCE), SnS3 (-0.5 to -0.81 V/SCE) and SnS4 electrodes (-0.5 to -0.83 V/SCE).

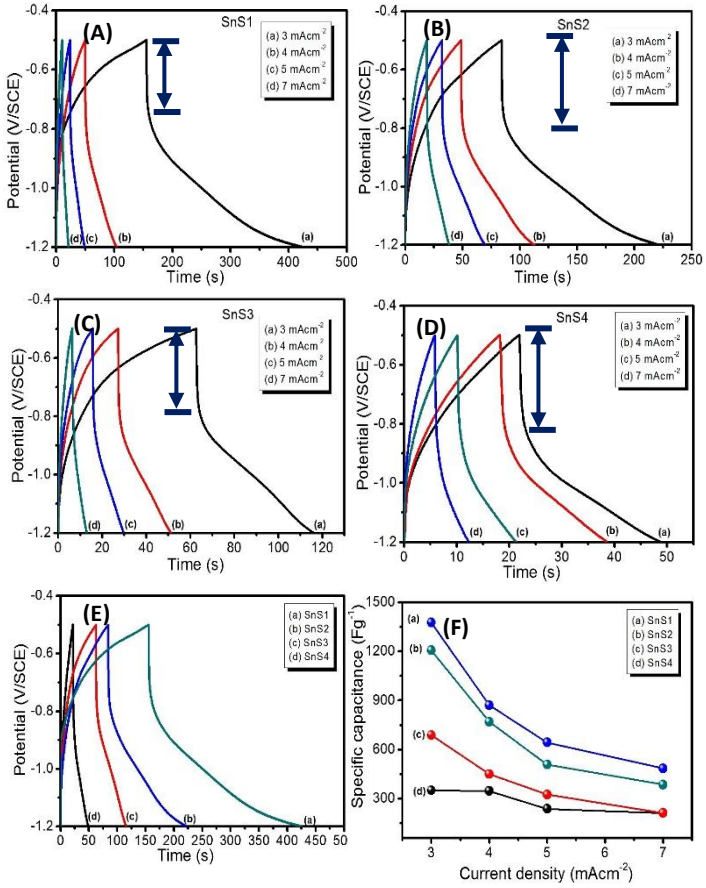

Figure 6: The GCD curves recorded at different current densities for (A) SnS1, (B) SnS2, (C) SnS3 and (D) SnS4 electrodes, respectively, (E) the comparative GCD curves of all electrodes at 3 mA cm^{-2}, and (F) the specific capacitance versus current density plot of all SnS thin films.

The slope shaped curves after -0.8 V/SCE indicated the pseudocapacitor behavior of SnS electrode. The C_s values are calculated using following equation as,

$$Cs = \frac{I \times t}{m \times \Delta V} \qquad (7)$$

Where, 'I' is the current density, 't' is discharging time, 'm' is a mass of material loaded at 1 cm^2 which is dipped in electrolyte and 'ΔV' is potential window. From GCD analysis, C_s values obtained for SnS1, SnS2, SnS3 and SnS4 electrodes as 1375, 1206, 688 and 350 F g^{-1}, respectively, at a constant current density of 3 mA cm^{-2}. The achieved values of specific capacitance is due to the micro-flower like structure of SnS thin film. The results reported ions this work is much higher than other previous reports, it is due to the higher specific surface area, surface morphology and the electrical conductivity of SnS electrode[14, 32, 33]. Figure 6 (E) shows the comparative GCD curves of SnS1, SnS2, SnS3 and SnS4 electrodes. The greater discharging rate of the SnS1 electrode proves the more charge storage ability of SnS1 electrode. The comparatively higher material interaction of electrode material with the OH^- ions from KOH electrolyte is because of the more time available for charge transfer at a lower current density. At a lower current density, the rate of intercalation is higher due to the total electrode material interaction. Also, the IR drop values for all electrodes increases with an increase in current density and the C_s values decreases correspondingly (Figure 6 (F)) [34].

Electrochemical stability and Ragone plot

The recyclability of SnS electrode material is tested by the CV cycling of electrode material at a scan rate of 100 mV s^{-1}. Figure 7 (A-D) shows the electrochemical stability of SnS1, SnS2, SnS3 and SnS4 electrode material upto 2000 CV cycles, respectively. The area under the CV curve does not decrease more even if 2000 CV cycles are completed, which indicates that the ability of electrode material in future supercapacitor. Figure 7(E)depicts the capacity retention versus cycle number plot of four electrode materials.The percent wise electrochemical stability of SnS1, SnS2, SnS3 and SnS4 electrode material is 89, 83, 76 and 75 %, respectively (Figure 7 (F)). The microstructure, adherence and higher surface area of SnS1 electrode material provide higher cycling stability.

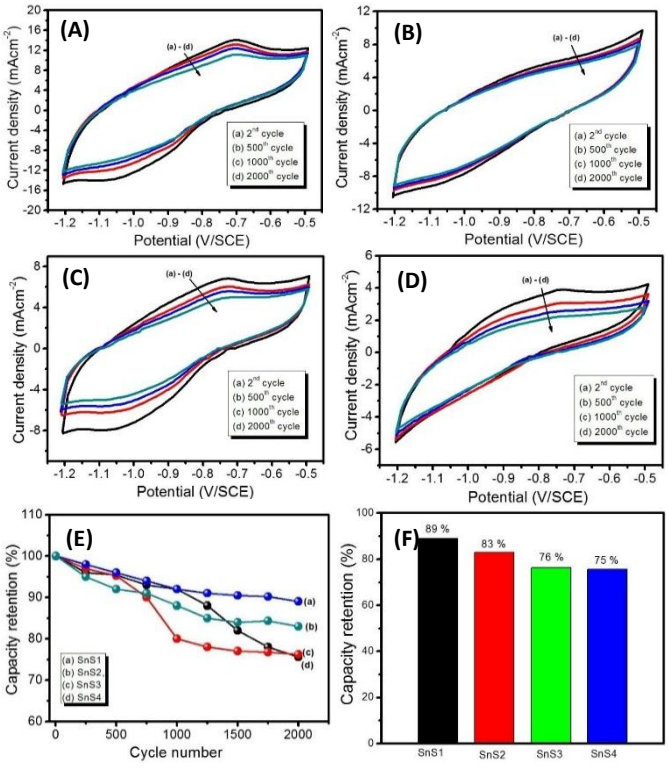

Figure 7: The CV curves at differentCV cycles in constant scan rate of 100 mV s^{-1} for (A) SnS1, (B) SnS2, (C) SnS3 and (D) SnS4 electrodes, (E) Capacity retention versus cycle number plot, and (F) Histogram of electrochemical stability of all four SnS electrodes.

Figure 8shows Ragone plots of SnS1, SnS2, SnS3 and SnS4 electrodes. The energy density decreases with an increase in the specific power density. The maximum energy densities obtained as 68, 60, 55 and 35 W h kg^{-1} and maximum power densities calculated as 8, 12, 10 and 3.5 kW kg^{-1}, respectively. These thin film materials fix the position between ordinary capacitor and batteries region in Ragone plot.

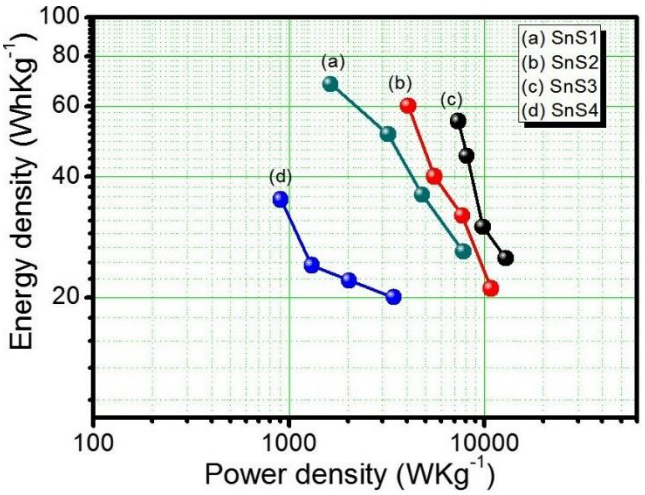

Figure 8: Ragone plots of SnS1, SnS2, SnS3 and SnS4 electrodes.

EIS analyses

Figure 9 shows the impedance plots of SnS1, SnS2, SnS3 and SnS4 electrodes in the frequency range of 1 kHz to 1 MHz at a bias potential of 10 mV. The inset figure shows the equivalent circuit diagram from which the Nyquist plot is fitted. The Nyquist plots of all SnS electrode shows the semicircle at higher frequency region. The intercept on the real axis gives equivalent series resistance (ESR) of an electrode material which consists of electronic and ionic contributions [35]. The electronic resistance is connected to the electronic resistance of the SnS particles and resistance between SnS electrode material and current collector. The ionic resistance is related to the KOH electrolyte resistance.

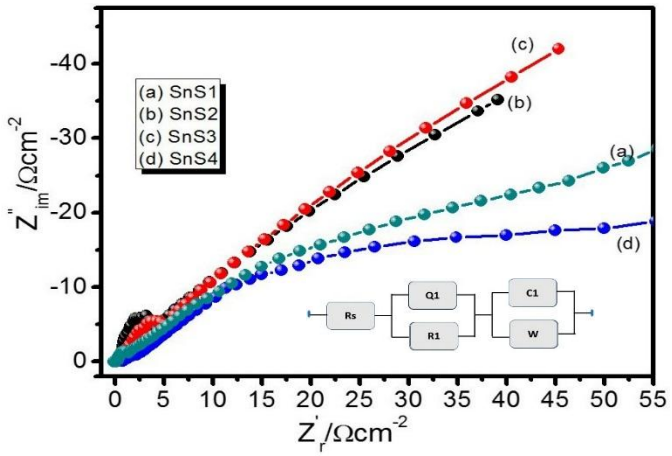

Figure 9: Nyquist plots of SnS1, SnS2, SnS3 and SnS4 electrodes (Inset shows best fitted equivalent circuit).

The ESR of SnS1, SnS2, SnS3 and SnS4 nanostructures electrodes are calculated to be 0.18, 0.34, 0.48 and 0.85 Ωcm^{-2}, respectively. The lower ESR values owing to the highly porous nano-structure, which delivers low impedance and provide easy access to electrolyte ions for intercalation and deintercalation. The diameter of semicircle gives the charge transfer resistance (R_{ct}). The R_{ct} of 1.19, 3.88, 4.66 and 1.85 Ωcm^{-2} are observed for SnS1, SnS2, SnS3 and SnS4 electrodes, respectively. The diffusion of Sn^{2+} in KOH electrolyte gives a straight line after semicircle at 45º, which indicates the Warburg's constant (W). The SnS1 electrode shows lower impedance than other electrodes. Hence, from these analyses, the nano-flower morphological SnS1 electrode is suitable for supercapacitor.

Conclusions

In summary**,** the nano-flower morphological SnS thin films are successfully synthesized by the CBD method at different reaction time. The excellent C_s of 1375 F g^{-1} and S_{ED} and S_{PD} of 68 Wh kg^{-1} and 12 kW kg^{-1}, respectively, achieved with capacity retention of 89 % up to 2000 CV cycles for SnS1 electrode. This electrochemical investigations indicates the SnS as a future electrode material.

Acknowledgement

Present work was sustained by the Human Resources Development program (No. 20124010203180) of Korea Institute of Energy Technology Evaluation. The basic Science Research Program through the National Research Foundation of Korea (NRF) funded by the Ministry of Science, ICT (NRF-2015R1A2A2A01006856).

References

[1] P. Simon, Y. Gogotsi, Nat. Mater. "Materials for electrochemical capacitors", Vol. 7, pp. 845−854, 2008.

[2] H.L Wang, Y.Y Liang, T. Mirfakhrai, Z. Chen, H.S Casalongue, H.J Dai, "Advanced asymmetrical supercapacitors based on graphene hybrid materials", Nano Res, Vol. 4, pp. 729-736, 2011.

[3] A. M. Patil, A. C. Lokhande, N.R. Chodankara, P. A. Shinde, J. H. Kim, C.D. Lokhande, "Interior design engineering of CuS architecture alteration with rise in reaction bath temperature for high performance symmetric flexible solid state supercapacitor". J Industrial and Engineering chemistry, Vol. 46, pp. 91-102, 2017.

[4] S. Ye, J. Feng, P. Wu, "Deposition of Three-Dimensional Graphene Aerogel on Nickel Foam as a Binder-Free Supercapacitor Electrode". ACS Appl. Mater. Interfaces, Vol. 5, pp. 7122-7129, 2013.

[5] A. M. Patil, V. C. Lokhande, A. C. Lokhande, N. R. Chodankar, T. Ji, J. H. Kim, C. D.

Lokhande,"Ultrathin nickel sulfide nano-flames as an electrode for high performance supercapacitor; comparison of symmetric FSS-SCs and electrochemical SCs device". RSC Adv, Vol. 6, pp. 68388-68401, 2016.

[6] L.Q Mai, F. Yang, Y.L Zhao, X. Xu, L. Xu, Y.Z Luo, "Hierarchical MnMoO(4)/CoMoO(4) heterostructured nanowires with enhanced supercapacitor performance". Nat. Commun, Vol. 2, pp. 381-384, 2011.

[7] J.R Miller and P. Simon, "Electrochemical Capacitors for Energy Management". Science, Vol. 321, 651-652, 2008.

[8] S. Nardecchia, D. Carriazo, M.L Ferrer, M.C Gutierrez, F. del Monte, "Three dimensional macroporous architectures and aerogels built of carbon nanotubes and/or graphene: synthesis and applications". Chem. Soc. Rev, Vol. 42, pp. 794-830, 2013.

[9] E. Frackowiak and F. Beguin, "Carbon materials for the electrochemical storage of energy in capacitors". Carbon, Vol. 39, pp. 937-950, 2001.

[10] C. D. Lokhande, D. P. Dubal and O. S. Joo, "Metal oxide thin film based supercapacitors
". Curr. Appl. Phys, Vol. 11, pp. 255-270, 2011.

[11] M. Zhi, C. Xiang, J. Li, M. Li, N. Wu, "Nanostructured carbon–metal oxide composite electrodes for supercapacitors: a review". Nanoscale, Vol. 5, 72-88, 2013.

[12] X. Huang, X. Qi, F. Boey and H. Zhang, "Graphene-based composites". Chem. Soc. Rev, Vol. 41, pp. 666-686, 2012.

[13] T. Rath, L. Gury, I. Sánchez-Molina, L. Martínez, S. A. Haque, "Formation of porous SnS nanoplate networks from solution and their application in hybrid solar cells". Chem. Commun, Vol. 51, pp. 10198-10201, 2015.

[14] H. Chauhan, M.K. Singh, S.A. H.S Deka, "Synthesis of surfactant-free SnS nanorods by a solvothermal route with better electrochemical properties towards supercapacitor applications". RSC Adv, Vol.5, pp. 17228-17235, 2015.

[15] Z. Ma, Y. Wang, Y. Yang, M. Yousaf, M. Zou, Anyuan Cao, Ray P. S. Han, "Flexible hybrid carbon nanotube sponges embedded with SnS_2 from tubular nanosheaths to nanosheets as free-standing anodes for lithium-ion batteries". RSC. Adv, Vol. 6, pp. 30098-30105, 2016.

[16] X. Rui,H. Tan, Q. Yan, "Nanostructured metal sulfides for energy storage".Nanoscale, Vol. 6, pp. 9889-9924, 2014.

[17] L. Wang, Y. Ma, M. Yang, Y. Qi, "One-pot synthesis of 3D flower-like heterostructured SnS_2/MoS_2 for enhanced supercapacitor behavior". RSC Adv, Vol. 5, pp. 89069-89075, 2015.

[18] M. Sugiyama, T. Yokoi, A. Henmi, T. Asano, "Effect of Na on sulfurization growth of SnS thin films and solar cells using NaF/Sn-S precursor". Thin Solid Films, Vol. 615, pp. 25-28, 2016.

[19] H. Li, J. Jib, X. Zheng, Y. Ma, Z. Jin, H. Ji, "Preparation of SnS quantum dots for solar cells application by an in-situ solution chemical reaction process". Mater. Sci. Semicond. Process, Vol. 36, pp. 65-70, 2015.

[20] R. Tang, H. Su, Y. Sun, X. Zhang, L. Li, C. Liu, S. Zeng, D. Sun, "Enhanced photocatalytic performance in Bi_2WO_6/SnS heterostructures: Facile synthesis, influencing factors and mechanism of the photocatalytic process". J Colloid. Interf. Sci, Vol. 466, pp. 388-399, 2016.

[21] Y. Liu, H. Kang, L. Jiao, C. Chen, K. Cao, Y. Wang, H. Yuan, "Exfoliated-SnS_2 restacked on graphene as a high-capacity, high-rate, and long-cycle life anode for sodium ion batteries". Nanoscale, Vol. 7, 1325-1332, 2015.

[22] A. Umar, M.S. Akhtar, G.N. Dar, M. Abaker, A. Al-Hajry, S. Baskoutas, "Visible-light-driven photocatalytic and chemical sensing properties of SnS_2 nanoflakes". Talanta, Vol. 114, pp. 183-190, 2013.

[23] R. Wang, X. Yan, J. Lang, Z. Zheng, P. Zhang, "A hybrid supercapacitor based on flower-like Co $(OH)_2$ and urchin-like VN electrode materials". J. Mater. Chem. A, Vol. 2, pp. 12724-12732, 2014.

[24] M. Zhi, C. Xiang, J. Li, M. Li, N. Wu, "Nanostructured carbon–metal oxide composite electrodes for supercapacitors: a review".Nanoscale, Vol. 5, pp. 72-88, 2013.

[25] C. Deng, X. Ge, H. Hu, L. Yao, C. Han, D. Zhao, "Template-free and green sonochemical synthesis of hierarchically structured CuS hollow microspheres displaying excellent Fenton-like catalytic activities". Cryst. Eng. Comm, Vol. 16, pp. 2738-2745, 2014.

[26] A.M. Patil, A.C. Lokhande, N.R. Chodankar, V.S. Kumbhar, C.D. Lokhande, "Engineered morphologies of β-NiS thin films via anionic exchange process and their supercapacitive performance". Mater. Des. Vol. 97, pp. 407-416, 2016.

[27] X. Zhang, W. Shi, J. Zhu, W. Zhao, J. Ma, S. Mhaisalkar, T. Maria, Y. Yang, H. Zhang, H.H Hng, Q. Yan, "Synthesis of porous NiO nanocrystals with controllable surface area and their application as supercapacitor electrodes". Nano Res, Vol. 3, pp. 643-652, 2010.

[28] G.S. Gund, D.P. Dubal, S.B. Jambure, S.S. Shinde, C.D. Lokhande, "Temperature influence on morphological progress of Ni(OH)2 thin films and its subsequent effect on electrochemical supercapacitive properties". J. Mater. Chem. A, Vol. 1, pp. 4793-4803, 2013.

[29] H. Peng, G. Ma, K. Sun, J. Mu, H. Wang, Z. Lei, J. Mater. Chem. A, "High-performance supercapacitor based on multi-structural CuS@polypyrrole composites prepared by in situ oxidative polymerization". Vol. 2, pp. 3303-3307, 2014.

[30] S.K Meher, P. Justin, G.R Rao, "Nanoscale morphology dependent pseudocapacitance of NiO: Influence of intercalating anions during synthesis". Nanoscale, Vol. 3, pp. 683-692, 2011.

[31] H. Jiang, T. Zhao, C. Li, J.J Ma, "Hierarchical self-assembly of ultrathin nickel hydroxide nanoflakes for

high-performance supercapacitors". Mater. Chem, Vol. 21, pp. 3818-3823, 2011.

[32] Y. Li, H. Xie and J. Tu, Mater. Lett, "Nanostructured SnS/carbon composite for supercapacitor". Vol. 63, pp. 1785-1787, 2009.

[33] S. Sohila, M. Rajalakshmi, C. Muthamizhchelvan, S. Kalavathi, C. Ghosh, R. Divakar, C. N. Venkiteswaran, N. G. Muralidharan, A. K. Arora, E. Mohandas, "Synthesis and characterization of SnS nanosheets through simple chemical route". Mater. Lett, Vol. 65, pp. 1148-1150, 2011.

[34] S. Vijayakumar, S. Nagamuthu, G. Muralidharan, ACS Appl. Mater. Interfaces, 5 (2013) 2188.